Regular Article - Experimental Physics

Measurement of light mesons at RHIC by the PHENIX experiment

M. Naglis[a]
for the PHENIX Collaboration

Weizmann Institute of Science, Rehovot 76100, Israel

Abstract The PHENIX experiment at RHIC has measured a variety of light neutral mesons (π^0, K_S^0, η, ω, η', ϕ) via multi-particle decay channels over a wide range of transverse momentum. A review of the recent results on the production rates of light mesons in p + p and their nuclear modification factors in d + Au, Cu + Cu and Au + Au collisions at different energies is presented.

1 Introduction

The suppression of high-p_T light mesons in ultra-relativistic heavy ion collisions, compared to expectations from scaled p+p results, is one of the most interesting findings at RHIC. Particles with high transverse momentum are believed to be produced by fragmentation of hard-scattered partons in the earliest stage of the collision. In nucleus-nucleus collisions, the scattered hard partons lose their energy while traversing the subsequently produced hot and dense matter leading to the phenomenon of jet-quenching. Medium-induced effects on high-p_T particle production can be quantified with the nuclear modification factor:

$$R_{AA}(p_T) = \frac{d^2N_{AA}/dydp_T}{(\langle N_{coll}\rangle/\sigma_{pp}^{inel}) \times d^2\sigma_{pp}/dydp_T}, \qquad (1.1)$$

where $d^2N_{AA}/dydp_T$ is the differential yield per event in nucleus-nucleus collisions, $\langle N_{coll}\rangle$ is the number of binary nucleon-nucleon collisions averaged over the impact parameter range of the corresponding centrality, and σ_{pp}^{inel} and $d^2\sigma_{pp}/dydp_T$ are the total and differential cross sections for inelastic p + p collisions, respectively. In the absence of medium-induced effects, the yield of high-p_T particles is expected to scale with $\langle N_{coll}\rangle$, resulting in $R_{AA} = 1$ at high-p_T. Contrary to the suppression of mesons, baryons are found to be enhanced in central Au + Au collisions at RHIC at intermediate transverse momenta ($1.5 < p_T < 4.5$ GeV/c) [1]. The difference in the behavior of mesons and baryons is still not well understood.

Precise knowledge of meson and baryon yields and their ratios as a function of transverse momentum and in different collision systems, provides a mean to investigate the dependence of hadron formation on particle mass and quark-flavor composition, and the mechanisms of jet production and quenching. The PHENIX experiment excels in measuring light neutral mesons via multi-particle decay channels. This paper presents a review of the light meson data obtained in p + p and heavy-ion collisions at different energies.

2 Experimental setup and data analysis

The PHENIX detector [2] at RHIC (Relativistic Heavy Ion Collider) has been designed to measure a broad variety of signals from heavy ion collisions. PHENIX is capable of measuring electrons, photons and hadrons in a large dynamic range. The tracking of charged particles and measurements of their momentum are accomplished by the high-resolution multi-wire proportional Drift Chambers (DC) and the first layer of Pad Chambers (PC1). The typical value of the momentum resolution is $\sigma(p_T)/p_T \approx 1.0\% p_T \oplus 1.1\%$. The energy of photons and electrons is measured by highly segmented lead-glass (PbGl) and lead-scintillator (PbSc) Electro Magnetic Calorimeters (EMCal) which have an energy resolution of $\sigma_{PbGl}(E)/E \approx 5.9\%/\sqrt{E} \oplus 0.8\%$ and $\sigma_{PbSc}(E)/E \approx 8.1\%/\sqrt{E} \oplus 2.1\%$, respectively. Charged hadron identification is based on the particle mass calculated from the momentum and the time-of-flight information derived from the TOF or EMCal subsystems and the Beam Beam Counters (BBC's). The TOF subsystem with a time resolution $\sigma \simeq 120$ ps and the PbSc part of the EMCal with $\sigma \simeq 500$ ps allow to achieve reliable pion-kaon separation

a e-mail: maxim.naglis@weizmann.ac.il

836

Eur. Phys. J. C (2009) 61: 835–840

in the p_T ranges 0.3–2.5 GeV/c and 0.3–1.0 GeV/c, respectively. The Zero Degree Calorimeters (ZDC's) and BBC's are dedicated subsystems that determine the collision vertex and event centrality and also provide the minimum bias (MB) interaction trigger. The results of data presented in this paper are based on data samples accumulated during p + p, d + Au, Cu + Cu and Au + Au collisions at $\sqrt{s_{NN}}$ = 200 GeV, p+p and Cu+Cu collisions at $\sqrt{s_{NN}}$ = 62.4 GeV, and Cu + Cu collisions at $\sqrt{s_{NN}}$ = 22.4 GeV. The MB trigger used for p + p, d + Au and Cu + Cu collisions requires a coincidence between the BBC's with at least one hit in each BBC arm. For Au + Au collisions the MB trigger requires a coincidence between the BBC's and ZDC's with at least two hits in each BBC arm, at least one neutron detected in each ZDC arm. Besides, PHENIX utilizes a hardware high-p_T photon/electron trigger (ERT) based on the analog sum of the signals of adjacent 4 × 4 EMCal towers in coinci-

dence with the MB trigger condition. All events used in the analysis are required to have the collision vertex position along the beam axis within 30 cm of the geometrical center of PHENIX.

A summary of the decay channels studied and data samples analyzed is given in Table 2.1. The procedure used to reconstruct the invariant mass spectra of π^0, K_S^0, η, η', ω mesons is as follows. All photon clusters measured in the EMCal in a given event are paired to form the invariant mass distribution. Pairs with invariant mass within two standard deviations from the π^0 (η) mass are considered as π^0 (η) candidates. Raw π^0 (η) yields are determined by subtracting the yield of combinatorial pairs estimated by pairing photon clusters from different events. Then, the selected π^0 (η) candidates are combined between themselves, or with other photon clusters, or with charged tracks, according to the decay modes listed in Table 2.1. The invariant mass

Table 2.1 Summary of analyzed decay channels and data samples. In Au + Au (p + p) collisions, the measurements of the ϕ meson were performed using two different analysis techniques referred to in text as "two kaons PID" and "no PID" ("one kaon PID" and "no PID"), respectively

Data sample	$\sqrt{s_{NN}}$ (GeV)	$\int Ldt$	Trigger	Decay mode	p_T (GeV/c)	Reference
Run-2 Au + Au	200	24 μb^{-1}	MB	$\eta \to \gamma\gamma$	2.25–9.5	[6]
Run-3 p + p	200	0.35 pb^{-1}	ERT	$K_S^0 \to \pi^0\pi^0$	2.5–6.5	[7]
			MB	$\eta \to \gamma\gamma$	2.75–11.0	[6]
			ERT	$\eta \to \pi^0\pi^+\pi^-$	3.0–8.0	[6]
			ERT	$\omega \to \pi^0\pi^+\pi^-$	2.75–9.25	[5]
			ERT	$\omega \to \pi^0\gamma$	2.5–6.5	[5]
Run-3 d + Au	200	2.74 nb^{-1}	ERT	$K_S^0 \to \pi^0\pi^0$	3.5–8.5	[7]
			MB	$\eta \to \gamma\gamma$	2.25–11.0	[6]
			ERT	$\eta \to \pi^0\pi^+\pi^-$	5.0–8.0	[6]
			ERT	$\omega \to \pi^0\pi^+\pi^-$	3.5–9.0	[5]
			ERT	$\omega \to \pi^0\gamma$	3.0–7.0	[5]
			MB	$\phi \to K^+K^-$	1.45–5.1	[9]
Run-4 Au + Au	200	241 μb^{-1}	MB	$\pi^0 \to \gamma\gamma$	1.25–19.0	[15]
			MB	$\omega \to \pi^0\gamma$	4.0–9.0	[7]
			MB	$\phi \to K^+K^-$	0.8–4.0	[8]
			MB	$\phi \to K^+K^-$	2.45–7.0	–
Run-5 p + p	200	3.78 pb^{-1}	MB/ERT	$\pi^0 \to \gamma\gamma$	0.625–19.0	[14]
			ERT	$K_S^0 \to \pi^0\pi^0$	2.25–10.0	[7]
			ERT	$\omega \to \pi^0\pi^+\pi^-$	2.25–13.0	[7]
			ERT	$\omega \to \pi^0\gamma$	2.5–11.0	[7]
			ERT	$\eta' \to \eta\pi^+\pi^-$	3.25–10.75	–
			MB	$\phi \to K^+K^-$	0.9–4.5	–
			MB	$\phi \to K^+K^-$	1.3–7.0	–
Run-5 Cu + Cu	200	3.06 nb^{-1}	MB/ERT	$\pi^0 \to \gamma\gamma$	1.25.0–11.0	[12]
	62.4	0.19 nb^{-1}	MB	$\pi^0 \to \gamma\gamma$	1.25–7.5	[12]
	22.4	2.7 μb^{-1}	MB	$\pi^0 \to \gamma\gamma$	1.25–4.75	[12]
Run-6 p + p	62.4	0.1 pb^{-1}	MB/ERT	$\pi^0 \to \gamma\gamma$	0.625–6.75	[12]

Eur. Phys. J. C (2009) 61: 835–840

837

spectra of the ϕ meson are constructed using three different techniques. The first does not require track identification in the final state and assumes that all tracks are kaons ("no PID"). The second requires identification of only one kaon in the TOF subsystem ("one kaon PID"). In the third technique both kaons are identified in the TOF or EMCal subsystems ("two kaons PID"). Kaon candidates with opposite charge are combined to form the invariant mass distribution. Mass distributions obtained by the procedures described above contain both the signal and an inherent combinatorial background. Meson raw yields were extracted by simultaneously fitting the signal and background, or by integrating the spectra in the vicinity of the meson masses after subtraction of the combinatorial background, estimated using an event-mixing technique. Representative examples of the K^+K^- invariant mass distributions obtained using "no PID", "one kaon PID" techniques in p + p collisions and using "no PID" technique in 0–10% most central Au + Au collisions, and an example of the $\eta\pi^+\pi^-$ invariant mass distribution are shown in Fig. 2.1. Solid lines are fits to a sum of a Gaussian convoluted Breit-Wigner function to account

for the ϕ signal, or a pure Gaussian for the η' signal, and a polynomial background function. Corrections to the raw yields for the limited detector acceptance and resolution, reconstruction and trigger efficiency, multiplicity effects and various analysis cuts are determined from the full single-particle Monte Carlo simulation and analysis of the data.

3 Results

3.1 Particle spectra

The study of inclusive particle production in nucleon-nucleon collisions is a rich source of information on the fragmentation properties of partons in perturbative QCD and hadronization mechanisms. The PHENIX experiment has measured a variety of mesons in p + p collisions at $\sqrt{s} = 200$ GeV. These data in comparison to existing leading- and next-to-leading order perturbative QCD calculation can be used to constrain the model parameters. A compilation of published and preliminary results on meson production in p + p collisions is presented in Fig. 3.1. The different symbols for a given meson correspond to different decay channels or different analysis techniques. The third set of points from the bottom represents the first measurement of $\eta' \to \eta\pi^+\pi^-$ at RHIC at high-p_T. The solid lines shown in the figure are just to guide the eye.

The ϕ meson invariant p_T spectra measured in p + p, d + Au and Au + Au collisions at $\sqrt{s_{NN}} = 200$ GeV are
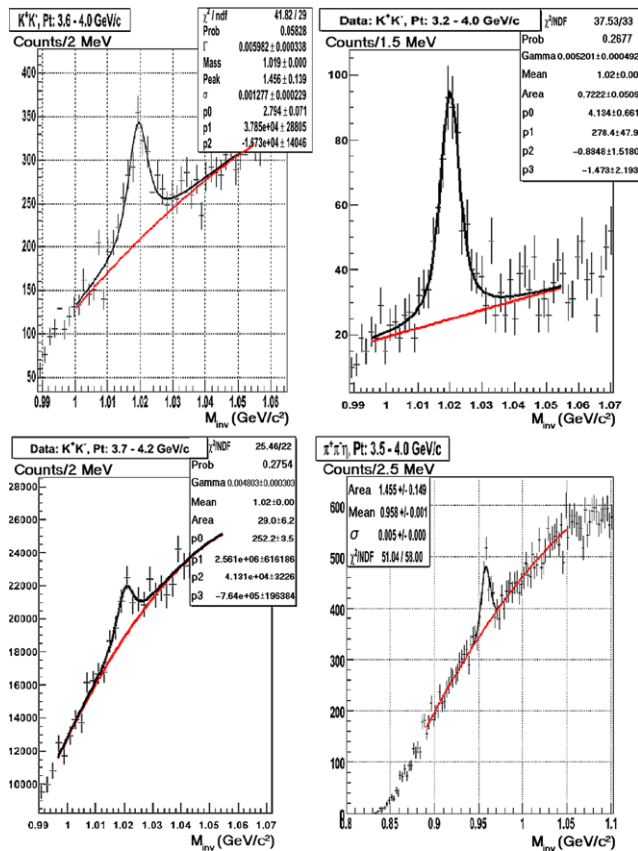

Fig. 2.1 Invariant mass distributions of the ϕ mesons reconstructed in the K^+K^- decay channel using "no PID" (*top left*), "one kaon PID" (*top right*) techniques in p + p collisions and using "no PID" (*bottom left*) technique in 0–10% most central Au + Au collisions. Invariant mass distribution of the η' mesons reconstructed in the $\eta\pi^+\pi^-$ decay channel (*bottom right*) in p + p collisions
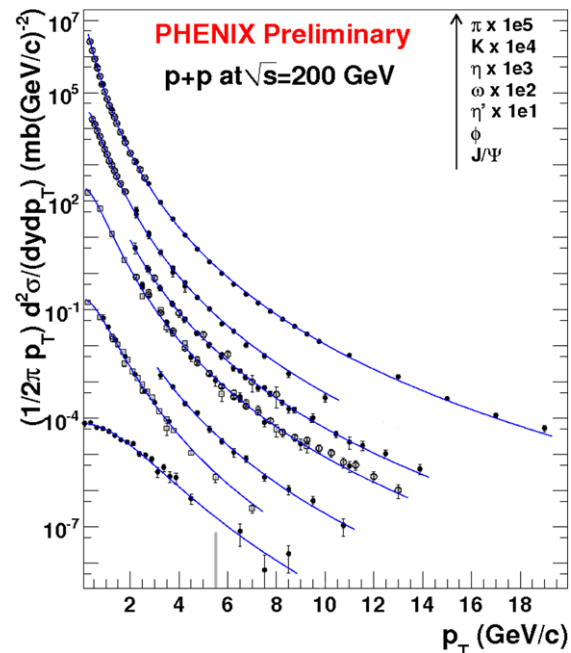

Fig. 3.1 Compilation of PHENIX results on meson production in p+p collisions at $\sqrt{s} = 200$ GeV. The *solid lines* are just to guide the eye. Charged kaon and pion data are taken from [3], J/Ψ data are taken from [4]

838

Eur. Phys. J. C (2009) 61: 835–840

Fig. 3.2 Invariant p_T spectra of ϕ meson measured in p + p, d + Au and Au + Au collisions at $\sqrt{s_{NN}} = 200$ GeV
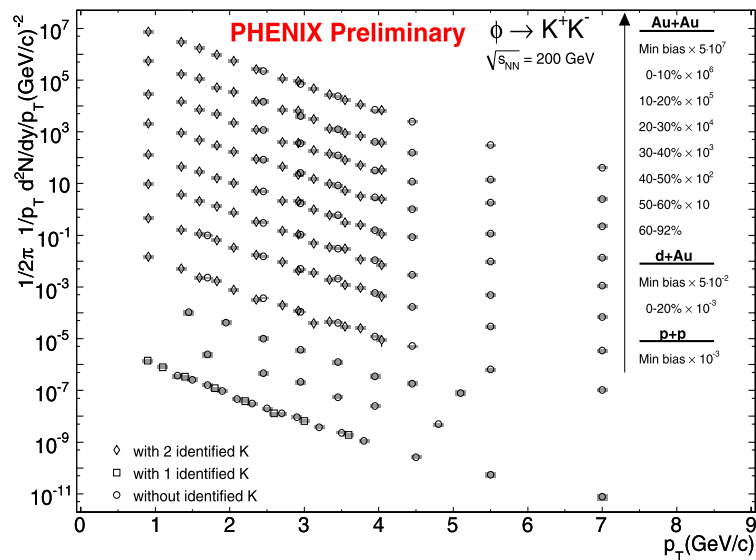
Table 3.1 Results of the fits to a constant for η/π^0, K_S^0/π^0 and ω/π^0 ratios in p + p and d + Au collisions at $\sqrt{s_{NN}} = 200$ GeV

System	η/π^0	K_S^0/π^0	ω/π^0
p + p	$0.48 \pm 0.02(\text{stat}) \pm 0.02(\text{syst})$	$0.45 \pm 0.01(\text{stat}) \pm 0.05(\text{syst})$	$0.81 \pm 0.03(\text{stat}) \pm 0.07(\text{syst})$
d + Au	$0.47 \pm 0.02(\text{stat}) \pm 0.02(\text{syst})$	$0.58 \pm 0.06(\text{stat}) \pm 0.05(\text{syst})$	$0.94 \pm 0.08(\text{stat}) \pm 0.12(\text{syst})$

shown in Fig. 3.2. As compared to the previously reported Au + Au results [8] obtained with the "two kaons PID" approach, the new "no PID" analysis extends the range of the measurements to higher p_T up to 7 GeV/c. In turn, the new "one kaon PID" analysis of p + p data extends the range of the "no PID" measurements reported in [9] to lower p_T down to 0.9 GeV/c. In spite of the very different sources of systematic uncertainties, the results of the "no PID" analysis are in good agreement with the results of "one kaon PID" and "two kaons PID" in p + p and Au + Au collisions, respectively. The combined p + p results of the "one kaon PID" and "no PID" analyses constitute a new p + p reference for ϕ meson, which supersedes the one used previously [8] having both a wider p_T range and smaller error bars.

The details of the K_S^0, η and ω measurements in p + p, d + Au and Au + Au collisions at $\sqrt{s_{NN}} = 200$ GeV can be found elsewhere [5–7]. Good agreement was obtained in the measurements of the same meson via two different decay channels, $\omega \to \pi^0\pi^+\pi^-$ or $\omega \to \pi^0\gamma$ and $\eta \to \pi^0\pi^+\pi^-$ or $\eta \to \gamma\gamma$. Analyses of MB and ERT data samples collected in Run-3 and Run-5 gave consistent results.

3.2 Particle ratios

Non-identical particle ratios measured at high-p_T are useful to assess the particle composition of jet fragmentation.

In p + p collisions, meson-to-meson ratios (η/π^0, K/π^0, η'/π^0, ω/π^0, ϕ/π^0, ϕ/K) derived using a parameterization of the π^0 invariant p_T spectra [10] exhibit a universal flat behavior above $p_T = 2.5$ GeV/c [9] indicating that the measured transverse momentum spectra for all light mesons have the same slope at high-p_T. Similarly to p + p results, η/π^0, K_S^0/π^0 and ω/π^0 ratios in d + Au collisions are also found to be flat in the same p_T range. Results of the fits to a constant performed in the p_T region above 2.5 GeV/c for η/π^0, K_S^0/π^0 and ω/π^0 ratios are presented in Table 3.1. As one can see, the results obtained in p + p and d + Au collisions are consistent within errors for the same ratio, indicating that the production of light mesons at $p_T > 2.5$ GeV/c is not affected by cold nuclear matter.

3.3 Nuclear modification factors

Using the new p + p reference, ϕ mesons's R_{AA} has been derived in central Au + Au collisions in the p_T range of 2.45–7 GeV/c. There is an ongoing work to extend this p_T range towards low-p_T. Figure 3.3 shows a comparison of the R_{AA} for ϕ mesons, other mesons (π^0, η, K, ω), protons and direct photons. Neutral pions and η mesons follow the same suppression pattern over the entire p_T range. The R_{AA} of ϕ mesons exhibits less suppression than η and π^0 in the p_T range of $2.45 < p_T < 4.5$ GeV/c. At
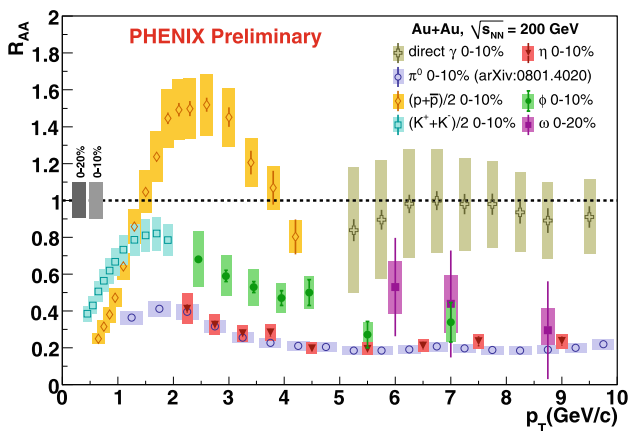
Fig. 3.3 Nuclear modification factor R_{AA} in central Au + Au collisions as a function of p_T for π^0, $(K^+ + K^-)/2$, η, ω, $(p + \bar{p})/2$, ϕ and direct γ. Direct γ data are taken from [11]

Fig. 3.4 (Color online) R_{AA} of π^0 as a function of transfer momentum in central Cu + Cu collisions at $\sqrt{s_{NN}} = 22.4$ GeV, 62.4 GeV and 200 GeV shown in *black*, *blue* and *red*, respectively. The *shaded bands* represent parton energy loss calculations [12]

higher p_T (>5 GeV/c) the amount of suppression of ϕ and ω could be similar to that of π^0 and η mesons. A more conclusive statement is not possible due to the large errors of the measurements. The similarity between the suppression patterns of different mesons at high-p_T favors the production of these mesons via jet fragmentation outside the hot and dense medium created in the collision. It is not clear whether the R_{AA} of charged kaons follow or not the trend of ϕ mesons, since the present measurements have no overlap in p_T. Interestingly, that R_{AA} of protons which are known to be enhanced in the intermediate p_T range [1], reach a value below unity at $p_T \approx 4.2$ GeV/c. Further investigations are required for understanding the influence of quark flavor composition on the suppression pattern.

3.4 Onset of jet quenching

In contrast to RHIC results at $\sqrt{s_{NN}} = 130$ GeV and 200 GeV, no suppression of high-p_T hadrons has been observed at SPS energies. This implies that there must be an intermediate value of collision energy at which the onset of high-p_T suppression happens. The results of a beam energy scan performed at RHIC with Cu + Cu collisions at $\sqrt{s_{NN}} = 22.4$ GeV, 62.4 GeV and 200 GeV, shown in Fig. 3.4, indicate that parton energy loss starts to dominate over Cronin enhancement at a center of mass energy somewhere between 22.4 and 62.4 GeV per nucleon pair [12]. Numerical calculations based on a parton energy loss model [13] describe well the suppression of π^0 mesons above $p_T = 3$ GeV/c at 62.4 GeV and 200 GeV. Measurements at 22.4 GeV favor the calculations carried out without taking into account parton energy loss.
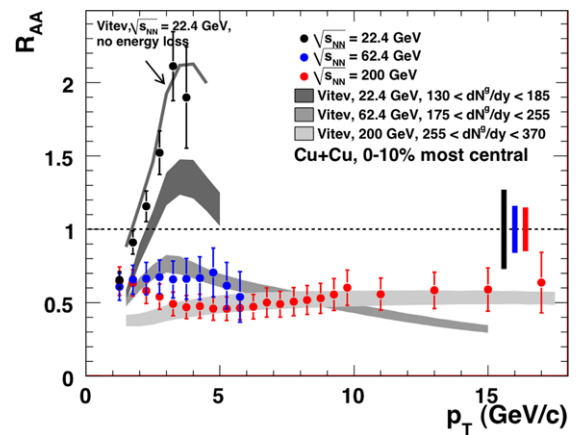
4 Summary and outlook

The PHENIX experiment at RHIC has performed a set of measurements of light mesons (π^0, K_S^0, η, ω, η', ϕ) via multi-particle decay channels at intermediate and high p_T in different collision systems. A first measurement of $\eta' \rightarrow \eta\pi^+\pi^-$ at RHIC performed by PHENIX at high-p_T is reported here. It would be very interesting to measure the production rate of η' in Au + Au collisions in view of predictions of a possible enhancement as its mass decreases in the hot and dense matter [16]. In p + p and d + Au p_T-dependent non-identical meson-to-meson ratios exhibit a universal flat behavior above $p_T = 2.5$ GeV/c demonstrating that p_T spectra of all measured light mesons have the same slope in this p_T range. Cold nuclear matter does not affect the production rates of light mesons at $p_T > 2.5$ GeV/c as seen from the matching of meson-to-meson ratios measured in p + p and d + Au. Using the new p + p reference, ϕ meson's R_{AA} has been derived in central Au + Au collisions. At intermediate-p_T ϕ meson is less suppressed than π^0 and η and it exhibits similar suppression level to those of π^0 and η at high-p_T. Parton energy loss calculations reproduce well the π^0 meson suppression for $p_T > 3$ GeV/c in Cu + Cu collisions at $\sqrt{s_{NN}} = 62.4$ GeV and 200 GeV. The onset of jet quenching is between 22.4 GeV and 62.4 GeV.

References

1. S.S. Adler et al., Phys. Rev. Lett. **91**, 172301 (2003)
2. K. Adcox et al., Nucl. Instrum. Methods A **499**, 469 (2003)
3. S.S. Adler et al., Phys. Rev. C **74**, 024904 (2006)

4. A. Adare et al., Phys. Rev. Lett. **98**, 232301 (2007)
5. S.S. Adler et al., Phys. Rev. C **75**, 051902 (2007)
6. S.S. Adler et al., Phys. Rev. C **75**, 024909 (2007)
7. V. Ryabov (PHENIX Collaboration), Int. J. Mod. Phys. E **16**, 1864 (2007)
8. D. Pal (PHENIX Collaboration), Nucl. Phys. A **774**, 489 (2006)
9. V. Ryabov (PHENIX Collaboration), J. Phys. G **35**, 044030 (2008)
10. S.S. Adler et al., Phys. Rev. Lett. **91**, 241803 (2003)
11. K. Reygers (PHENIX Collaboration), arXiv:0804.4562 [nucl-ex]
12. A. Adare et al., arXiv:0801.4555 [nucl-ex]
13. I. Vitev, Phys. Lett. B **639**, 38 (2006)
14. A. Adare et al., Phys. Rev. D **76**, 051106 (2007)
15. A. Adare et al., arXiv:0801.4020 [nucl-ex]
16. J.I. Kapusta et al., Phys. Rev. D **53**, 5028 (1996)